

Isothermal two-component stellar wind of hot stars

J. Krtička^{1,2} and J. Kubát²

¹ Katedra teoretické fyziky a astrofyziky PřF MU, Kotlářská 2, 611 37 Brno, Czech Republic

² Astronomický ústav, Akademie věd České republiky, 251 65 Ondřejov, Czech Republic

Received 13 December 1999 / Accepted 22 May 2000

Abstract. We present results of the solution of hydrodynamic equations of a two-component radiatively driven stellar wind with an inclusion of the frictional force. The temperature of the wind is assumed to be equal to the effective temperature of the star. We found that for the case of late B stars the stellar wind does not decouple, but its terminal velocity is lowered with respect to the one-component solution. This effect is a consequence of the radiative force dependence on the velocity gradient, which is inherent to the CAK model using the Sobolev approximation.

For hot B star and O stars there is no significant difference between one and two-component solutions.

Key words: stars: mass-loss – stars: winds, outflows – hydrodynamics – stars: early-type

1. Introduction

Radiatively driven wind in hot O stars may be adequately described using the model of Castor et al. (1975, hereafter CAK). One of the simplifying assumptions of this model is the usage of a one-fluid description of such wind, although the radiative force acts mostly on metallic ions. Castor et al. (1976) showed that possible drift velocity between absorbing ions and protons is not a serious problem. However, the majority of the calculations that followed the introduction of the CAK theory was performed for O stars, where the gas can be really considered as a one component. The possibility that the wind could be considered as a multicomponent one for stars cooler than O was raised by Springmann & Pauldrach (1992, hereafter SP) who intended mainly to obtain a modified temperature structure of such a wind rather than obtain a solution of hydrodynamic equations.

A great stride was made by Babel (1995) who solved multicomponent hydrodynamic equations of stellar wind for main sequence A star. Porter & Drew (1995) studied decoupling in the outflow from B stars. However, they did not solve the hydrodynamic equations, they rather supposed a beta velocity law. Recently, Porter & Skouza (1999) using the theory of the decoupled wind pointed out the possibility of the presence of pulsating

shells around stars with low-density radiatively driven wind and Hunger & Groote (1999) studied the decoupling of helium in a stellar wind. In this paper (similarly to Babel 1995, 1996) we aim at self-consistent calculation of both density and velocity structure of different components of stellar wind.

2. Description of the model

We assume that the star has a stationary spherically symmetric isothermal ($T_{\text{wind}} = T_{\text{eff}}$) wind consisting of two ideal gas components, namely of hydrogen ions with mass equal to proton mass m_p and charge equal to proton charge q_p (hereafter called passive plasma) and of absorbing ions with mass $A_i m_p$ and charge q_i . We assume that passive plasma does not absorb any radiation. On the other hand, ions receive all the radiative acceleration.

2.1. Model equations

We start with the basic hydrodynamic equations describing our two-component wind, namely with the continuity equations

$$\frac{d}{dr} (r^2 \rho_p v_{rp}) = 0, \quad (1a)$$

$$\frac{d}{dr} (r^2 \rho_i v_{ri}) = 0, \quad (1b)$$

and with the equations of motion (cf. Braginskij 1963)

$$v_{rp} \frac{dv_{rp}}{dr} = -g + \frac{1}{\rho_p} R_{pi} - \frac{1}{\rho_p} \frac{dp_p}{dr}, \quad (2a)$$

$$v_{ri} \frac{dv_{ri}}{dr} = g_i^{\text{rad}} - g - \frac{1}{\rho_i} R_{pi} - \frac{1}{\rho_i} \frac{dp_i}{dr}. \quad (2b)$$

In these equations v_{rp} , v_{ri} are velocities of passive plasma and accelerated ions, respectively, ρ_p , ρ_i are densities of passive plasma and absorbing ions, respectively, p_p , p_i are partial gas pressures of each component ($p_p = a_p^2 \rho_p = (kT/m_p) \rho_p$, $p_i = a_i^2 \rho_i = (kT/m_i) \rho_i$), $g = G\mathfrak{M}(1 - \Gamma)/r^2$ is the gravitational acceleration acting on each component (G and \mathfrak{M} are gravitational constant and stellar mass, respectively, Γ is the Eddington factor that reduces the gravity on the absorption on free electrons) and g_i^{rad} is the radiative acceleration acting on

absorbing ions. We take the radiative acceleration in the form

$$g_i^{\text{rad}} = \frac{1}{\mathfrak{Y}_i} \frac{\sigma_e L}{4\pi r^2 c} f \left(\frac{n_e/W}{10^{11} \text{cm}^{-3}} \right)^\delta k \left(\frac{\mathfrak{Y}_i}{\sigma_e v_{\text{th}} \rho_i} \frac{dv_{r_i}}{dr} \right)^\alpha, \quad (3)$$

with force multipliers k , α , δ after Abbott (1982). Here f is the finite disk correction factor (Pauldrach et al. 1986, Friend & Abbott 1986), n_e is the electron density (we put $n_e = n_p$), and W is stellar dilution factor. Eq. (3) is commonly used for a description of the radiative acceleration for a one-component wind. However, since the same radiative force directly accelerates different amount of matter (only ions), the corresponding acceleration is modified. The Abbott's parametrisation using k , α , and δ was originally introduced only for a one-component wind and if we want to use it for the case of a two-component wind, we must introduce some scaling. To fulfil this requirement we introduced the quantity \mathfrak{Y}_i , which is the ratio of the absorbing ions density to the passive plasma at the inner boundary of the wind.

Frictional force (per unit volume) R_{pi} acting between both components has the form (SP):

$$R_{\text{pi}} = n_p n_i k_{\text{pi}} G(x_{\text{pi}}), \quad (4)$$

where n_p and n_i are number densities of passive plasma and absorbing ions. The friction coefficient k_{pi} is given by

$$k_{\text{pi}} = \frac{4\pi \ln \Lambda q_p^2 q_i^2}{kT} \frac{v_{r_p} - v_{r_i}}{|v_{r_p} - v_{r_i}|}, \quad (5)$$

where $\ln \Lambda$ is the Coulomb logarithm, $G(x)$ is the so-called Chandrasekhar function, which is defined in terms of the error function $\Phi(x)$ (see Dreicer 1959)

$$G(x) = \frac{1}{2x^2} \left(\Phi(x) - x \frac{d\Phi(x)}{dx} \right). \quad (6)$$

The argument x_{pi} of the Chandrasekhar function in Eq. (4) is proportional to the ratio of the drift velocity $|v_{r_p} - v_{r_i}|$ to the thermal velocity v_{th} , namely

$$x_{\text{pi}} = \sqrt{A_{\text{pi}}} \frac{|v_{r_p} - v_{r_i}|}{v_{\text{th}}},$$

where $A_{\text{pi}} = A_p A_i / (A_p + A_i)$ is a reduced atomic mass.

2.2. Critical points

Critical points of the CAK stellar wind model were thoroughly discussed by Abbott (1980). Our results are similar to that computed for the three-fluid model by Bürgi (1992).

Two-component radiatively driven stellar wind should have a critical point for each of the components. The one for the passive plasma is similar to that known from coronal wind and it is given by the condition

$$v_{r_p} = a_p. \quad (7)$$

The second critical point is the critical point for ions

$$v_{r_i} - \frac{a_i^2}{v_{r_i}} - \frac{\partial g_i^{\text{rad}}}{\partial (dv_{r_i}/dr)} = 0. \quad (8)$$

This condition is the CAK condition for pure ion gas. Alternatively, we can use the common critical point condition for a one-component wind. Equation of motion for a one-component wind with the help of our definition of radiative acceleration reads

$$v_r \frac{dv_r}{dr} = \frac{a^2}{v_r} \frac{dv_r}{dr} + \frac{2a^2}{r} + \mathfrak{Y}_i g_i^{\text{rad}} - g.$$

This equation has a singular point, so called CAK critical point, defined by the condition

$$v_r - \frac{a^2}{v_r} - \mathfrak{Y}_i \frac{\partial g_i^{\text{rad}}}{\partial (dv_r/dr)} = 0. \quad (9)$$

This condition for the one-component CAK critical point can be put to more convenient form using individual equations of motion (2a) and (2b). First, we annihilate friction terms in these equations by multiplying each equation by a corresponding density and summing of obtained equations,

$$\begin{aligned} \rho_p \left(v_{r_p} - \frac{a_p^2}{v_{r_p}} \right) \frac{dv_{r_p}}{dr} + \rho_i \left(v_{r_i} - \frac{a_i^2}{v_{r_i}} \right) \frac{dv_{r_i}}{dr} = \\ \rho_i g_i^{\text{rad}} + \frac{2\rho_p a_p^2}{r} + \frac{2\rho_i a_i^2}{r} - g(\rho_p + \rho_i), \end{aligned} \quad (10)$$

where continuity equations Eq. (1a) and (1b) were used. The corresponding critical point condition may be expressed as

$$\begin{aligned} \rho_p \left(v_{r_p} - \frac{a_p^2}{v_{r_p}} \right) \frac{dv_{r_p}}{dr} + \rho_i \left(v_{r_i} - \frac{a_i^2}{v_{r_i}} - \frac{\partial g_i^{\text{rad}}}{\partial (dv_{r_i}/dr)} \right) \\ \times \frac{dv_{r_i}}{dr} = 0. \end{aligned} \quad (11)$$

In the one-component limit (when $v_{r_p} \approx v_{r_i}$ and $dv_{r_p}/dr \approx dv_{r_i}/dr$) the Eq. (11) reduces to the Eq. (9). Therefore we use condition (11) to obtain the mass-loss rate of our models.

2.3. Boundary conditions

We start to calculate our models at a passive plasma critical point $r = R_*$ at the stellar surface. The passive plasma velocity at this point is

$$v_{r_p}(R_*) = a_p. \quad (12)$$

Velocity of ions can be obtained from Eq. (2a), which reduces to

$$g = \frac{2a_p^2}{r} + \frac{1}{\rho_p} R_{\text{pi}} \quad (13)$$

at the passive plasma critical point. We assume, that at a point r_{at} deep in the atmosphere where the velocities of both components are equal $\rho_i(r_{\text{at}}) = \mathfrak{Y}_i \rho_p(r_{\text{at}})$. We have chosen the value of $\mathfrak{Y}_i = 0.0127$, which corresponds to solar abundances of chemical elements. Using the continuity equations for both components we have

$$\rho_p(R_*) = \frac{1}{\mathfrak{Y}_i} \rho_i(R_*) \frac{v_{r_i}(R_*)}{v_{r_p}(R_*)} \quad (14)$$

used as a boundary condition for passive plasma density. Metallic ion density $\rho_i(R_*)$ is chosen to match the CAK solution for ions (see Sect. 2.4).

2.4. Method of solution

To solve the problem described here, we need a numerical method which is capable to solve a set of coupled nonlinear differential equations. We selected the Henyey method (Henyey et al. 1964), which was already used to solve the equations of a radiatively driven stellar wind by Nobili & Turolla (1988).

The set of the Eqs. (1a,1b,2a, 2b), which must be solved, may be formally written as

$$\mathbf{P}\psi = 0, \quad (15)$$

where the vector of the variables is used in the form (NR is the number of grid points)

$$\psi = (\rho_{i1}, v_{ri1}, \rho_{p1}, v_{rp1}, \rho_{i2}, v_{ri2}, \rho_{p2}, v_{rp2}, \dots, \dots, \rho_{iNR}, v_{riNR}, \rho_{pNR}, v_{rpNR}). \quad (16)$$

Solution of Eq. (15) is obtained using the iterative scheme

$$\delta\psi^{n+1} = -(\hat{J}^n)^{-1} \mathbf{P}^n \psi^n, \quad (17)$$

where ψ^n is solution in the n -th iteration and \hat{J}^n is the Jacobian in the n -th iteration,

$$\hat{J}_{kl}^n = \frac{\partial P_k}{\partial \psi_l}. \quad (18)$$

To solve this system of equations we use numerical package LAPACK, developed at the University of Tennessee.

We use exponential grid with accumulation of grid points near the photosphere. We approximate derivatives in each grid point by interpolating of the derivatives in the middle between grid points, except the outer boundary where the value for the last midpoint is used. Detailed form of the operator \mathbf{P} is given in Appendix.

We start our solution with a first estimate of both velocities (v_{ri} and v_{rp}) after the beta-velocity law $v_r = v_\infty(1 - R_*/r)^\beta$ with $\beta \approx 0.5-1.0$. The velocities at the lower boundary are set according to the Eqs. (12) and (13). In addition, we choose the boundary value $\rho_{i,1} = \rho_0^{(1)}$ (we choose low value of $\rho_0^{(1)}$ well below its expected CAK value) and $\rho_{p,1}$ is calculated using Eq. (14). The first guess of the density is computed from the continuity Eqs. (1a,1b).

Then the system of Eqs. (15) is solved using the Newton-Raphson method. If the procedure converges we check the left hand side of Eq. (11) for all depth points. If it is less than zero everywhere, we increase the lower boundary value of ρ_0 using the relation $\rho_0^{(n+1)} = (1+x)\rho_0^{(n)}$ ($x \approx 0.5$) and repeat the Newton-Raphson step. If the left hand side of Eq. (11) is greater than zero for some r or if the Newton-Raphson method fails to converge, we return one step back and set lower value of the lower boundary value of ρ_0 using the relation $\rho_0^{(n)} = (1+x/2)\rho_0^{(n-1)}$ and repeat the Newton-Raphson step. We stop our calculation when

Table 1. Adopted parameters of model stars

Stellar type	Stellar parameters			Wind parameters			Average ion	
	\mathfrak{M} [\mathfrak{M}_\odot]	R_* [R_\odot]	T_{eff} [K]	k	α	δ	q_i/q_p	A_i
B0	90.0	37.0	28 500	0.170	0.590	0.09	3.0	12.0
B5	4.36	3.01	15 500	0.235	0.511	0.12	2.0	12.0

our solution reaches the critical point defined by Eq. (11). It happens with sufficient accuracy when the difference between successive estimates of $\rho_0^{(n)}$ is less than 1%. Typically 10–20 iterations are sufficient to obtain CAK solution.

We determine the location of the CAK point as the point where the absolute value of the quantity on the left hand side of equation Eq. (11) has its minimum value. Then we start to compute the solution at the outer part of the wind using the same set of equations, however with Eqs. (A.1a)–(A.1d) replaced by equations where boundary values of each variable are equal its critical point values. Only one Newton-Raphson step is necessary to obtain the solution.

3. Results of calculations

Parameters of each model star are given in Table 1. Stellar parameters T_{eff} , \mathfrak{M} , R_* of a giant star of a spectral type B0 (corresponding to the star ϵ Ori) are taken from Pauldrach et al. (1986), parameters of a main sequence star of a spectral type B5 are taken from Harmanec (1988). We selected carbon in an appropriate ionization stage as a representative ion.

3.1. Star with high mass loss rate

We calculated a model of a two-component stellar wind for the case of an O6 star (see Krtička & Kubát 2000) and for a B0 star (see Fig. 1). We plotted the dependence of both ion and passive plasma velocities on radius in the wind. There are no significant differences between one-component and two-component models. This result has already been mentioned by SP (model of ζ Puppis therein). The mass-loss rate of both one-component and two-component models of a B0 star is $4.4 \cdot 10^{-6} \mathfrak{M}_\odot/\text{year}$.

3.2. Star with low mass loss rate

For stars with low mass-loss rate ($4.8 \cdot 10^{-12} \mathfrak{M}_\odot/\text{year}$) the situation changes (see Fig. 2). Beyond the CAK critical point near $r \approx 1.3R_*$ the velocity gradients of *both* components in a two component wind fall down. The reason for this strange behaviour may be explained as follows.

At a point where the maximum of the Chandrasekhar function is reached, the absolute value of the drift velocity $|v_{ri} - v_{rp}|$ is approximately equal to the thermal velocity v_{th} (i.e. $x_{pi} \approx 1$). In our particular case it happens for $r \approx 1.3R_*$ (see Fig. 3). There the frictional force R_{pi} (which is the accelerating force of passive plasma) starts to decrease rapidly – cf. Eqs. (4) and (6), the amount of momentum transferred to the

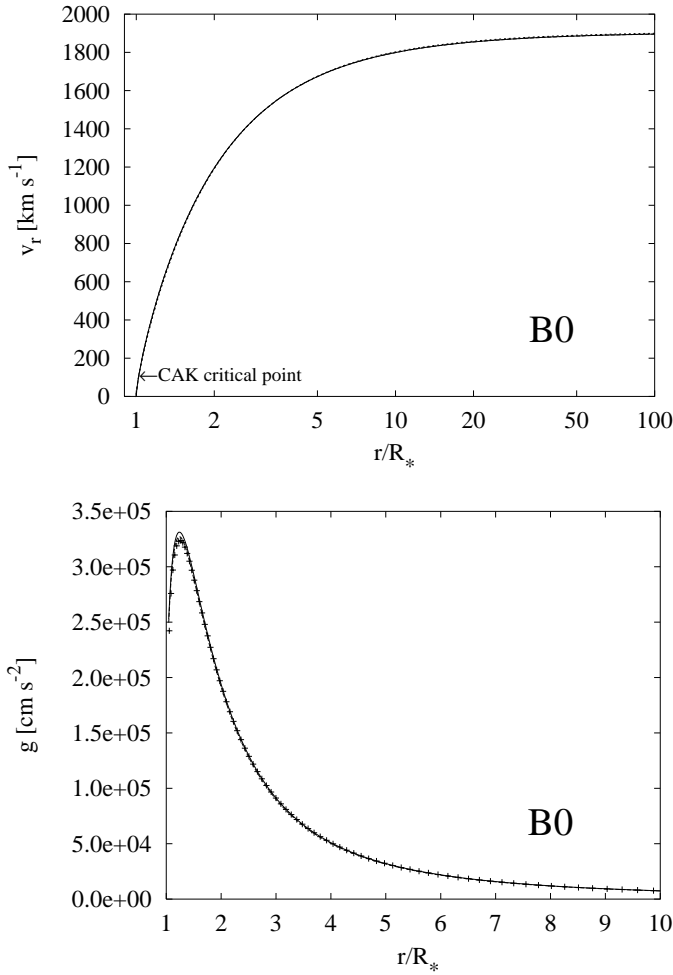


Fig. 1. *Upper panel:* one-component (dotted line) and two-component (radiatively accelerated ions – dashed line, passive plasma – full line) wind model of a B0 star. The ionic charge $q_i = 3$. The location of the CAK critical point is similar to that of critical point of two-component wind given by the condition (11). The CAK point of the both two-component and one-component wind is nearly the same. *Lower panel:* comparison of radiative acceleration acting on metals in a two-component model (full line), frictional acceleration acting on metals in a two-component model (dashed line), and radiative acceleration in one-component model scaled to metal density (crosses). Note that frictional acceleration is fully balanced by the radiative acceleration in two-component model and corresponds to the radiative acceleration in one-component model (see text).

passive plasma is lower, and, consequently, its *velocity gradient* abruptly falls.

However, there is a question, why the velocity of passive plasma still rises above this point. The reason is that the frictional force is larger than gravity throughout the wind. More deep insight into this problem can be obtained using the equation of motion (2a) and Eq. (4)

$$v_{rP} \frac{dv_{rP}}{dr} = -\frac{G\mathfrak{M}_{\text{eff}}}{r^2} - \frac{1}{\rho_P} \frac{dp_P}{dr}, \quad (19)$$

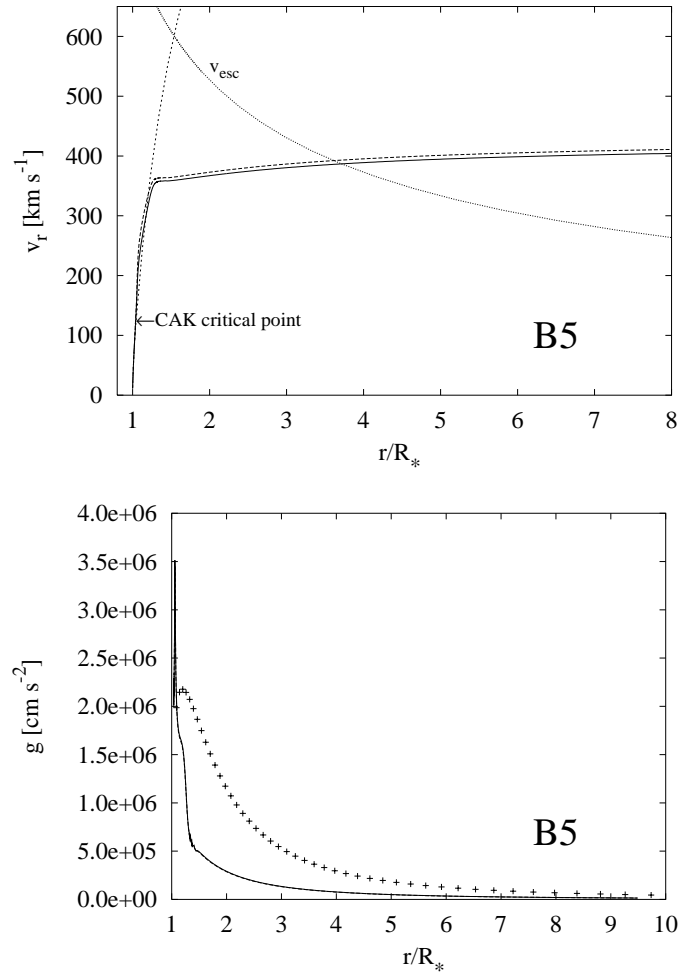


Fig. 2. The same as Fig. 1 for a B5 star. *Upper panel:* In addition, the escape velocity v_{esc} is plotted, too. The CAK point of the both two-component and one-component wind is nearly the same. *Lower panel:* Contrary to Fig. 1, the frictional and radiative accelerations differ from the one-component radiative acceleration (crosses).

where G is the gravitational constant and the effective mass $\mathfrak{M}_{\text{eff}}$ is introduced using the equation

$$\frac{G\mathfrak{M}_{\text{eff}}}{r^2} = \frac{G\mathfrak{M}}{r^2} - \frac{1}{\rho_P} R_{\text{pi}} \quad (20)$$

For our model of the two-component wind the second term at the right hand side of Eq. (20) is larger than the first one, and, consequently, $\mathfrak{M}_{\text{eff}}$ is negative. Eq. (19) is similar to the equation of the coronal wind, however the variable $\mathfrak{M}_{\text{eff}}$ is used instead of \mathfrak{M} . It follows that dv_{rP}/dr is positive. Consequently, passive plasma velocity rises also after abrupt fall of the velocity gradient.

Another question is: why are the absorbing ions bound to the passive plasma after maximum of frictional force is reached? For our particular case, $\rho_P \gg \rho_i$ and as it follows from Fig. 2 also $v_{rP} \approx v_{r_i}$ and $dv_{rP}/dr \approx dv_{r_i}/dr$. Eq. (10) takes the form

$$\rho_P v_{rP} \frac{dv_{rP}}{dr} = \rho_i g_i^{\text{rad}} - \rho_P g. \quad (21)$$

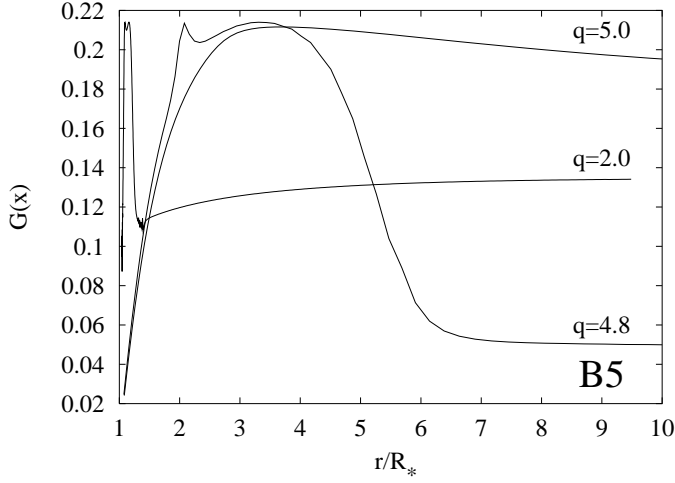


Fig. 3. The run of the Chandrasekhar function as a function of the radial coordinate r for models of a B5 star wind with different ionic charge. For the case of $q_i = 5.0$ the global maximum of the Chandrasekhar function is not reached, although the drift velocity is only slightly less than the thermal velocity. Contrary, in the case $q_i = 4.8$ the maximum of the Chandrasekhar function is reached (the local minimum appears because the drift velocity is greater than the drift velocity corresponding to the maximum value of the Chandrasekhar function). Similarly for $q_i = 2.0$.

It follows from the Eq. (21) that if the densities ρ_i and ρ_p vary slowly, the decrease of the gradient dv_{r_p}/dr causes decrease of the radiative acceleration g_i^{rad} and this means decrease of the dv_{r_i}/dr . Since the radiative acceleration depends explicitly on the velocity gradient dv_{r_i}/dr , its decrease causes further decrease of the radiative acceleration. This nonlinear effect leads to abrupt decrease of the velocity gradient.

Let us study the effect of lowering the ionic velocity gradient in more detail. Consider the momentum Eq. (2b) for the case of no difference between one-component and two-component solutions (our particular case of a B0 star – Fig. 1), namely

$$v_{r_i} \left. \frac{dv_{r_i}}{dr} \right|_1 = g_i^{\text{rad}} \Big|_1 - g - \frac{1}{\rho_i} R_{\text{pi}} \Big|_1, \quad (22)$$

where the gas pressure term was neglected again, and the subscript 1 stands for “one-component”. Now, let us assume that the frictional force is lowered by ΔR_{pi} ,

$$v_{r_i} \left. \frac{dv_{r_i}}{dr} \right|_2 = g_i^{\text{rad}} \Big|_2 - g - \frac{1}{\rho_i} (R_{\text{pi}} \Big|_1 - \Delta R_{\text{pi}}). \quad (23)$$

Subtracting Eqs. (23) and (22) and using the Taylor expansion of $g_i^{\text{rad}}(dv_{r_i}/dr)$ (we neglected all non-linear terms) we obtain

$$v_{r_i} \Delta \left. \frac{dv_{r_i}}{dr} \right| = \left. \frac{\partial g_i^{\text{rad}}}{\partial (dv_{r_i}/dr)} \right|_1 \Delta \left. \frac{dv_{r_i}}{dr} \right| + \frac{1}{\rho_i} \Delta R_{\text{pi}}, \quad (24)$$

where $\Delta dv_{r_i}/dr = dv_{r_i}/dr \Big|_2 - dv_{r_i}/dr \Big|_1$. Expressing the change of the metallic ion velocity gradient from the Eq. (24) we have

$$\Delta \left. \frac{dv_{r_i}}{dr} \right| = \frac{1}{\rho_i} \frac{\Delta R_{\text{pi}}}{v_{r_i} - \left. \frac{\partial g_i^{\text{rad}}}{\partial (dv_{r_i}/dr)} \right|_1}. \quad (25)$$

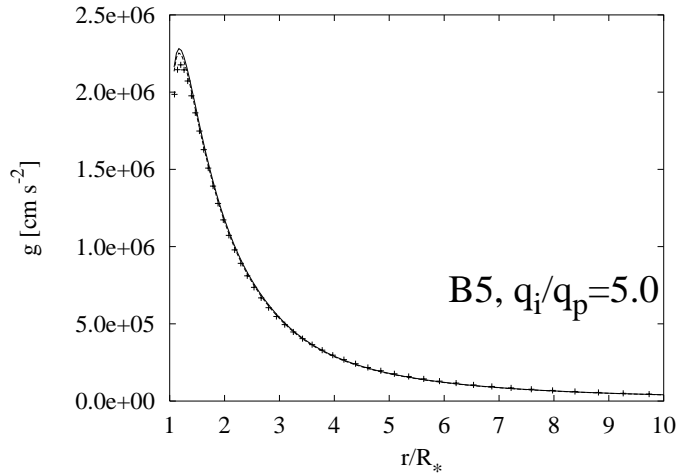
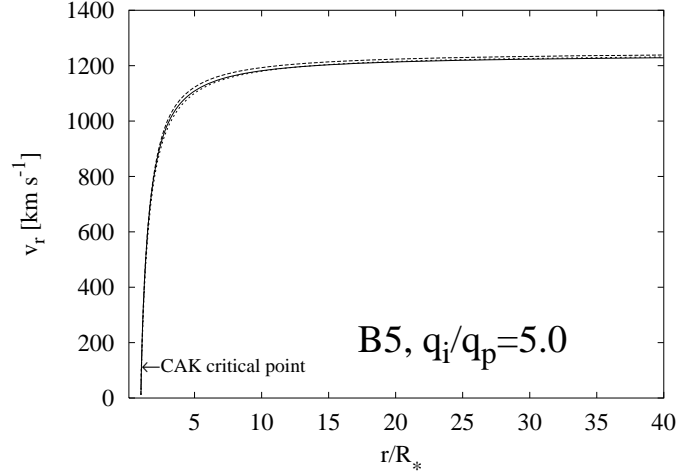


Fig. 4. Upper panel: the same as Fig. 2, but for $q_i = 5 q_p$. The CAK point of the both two-component and one-component wind is nearly the same. Lower panel: comparison of radiative acceleration acting on metals in two-component model (full line), frictional acceleration acting on metals in two-component model (dashed line), and radiative acceleration in one-component model scaled to metal density (crosses). Note that frictional acceleration is fully balanced by the radiative acceleration in two-component model and corresponds to radiative acceleration in one-component model (see text, compare with Fig. 5).

Since we are below the ionic critical point defined by the Eq. (8) (i.e. $v_{r_i} < \partial g_i^{\text{rad}} / \partial (dv_{r_i}/dr)$), and $\Delta R_{\text{pi}} > 0$, the change of the velocity gradient $\Delta (dv_{r_i}/dr)$ should be *negative*. Thus lowering the frictional force causes lowering of the ion velocity gradient. Consequently, absorbing ions are bound to the passive plasma and no runaway occurs.

This effect was enabled since we explicitly included the friction force and did not assume that the velocities of both components are equal. This effect is impossible in a one-component wind.

Finally, because the fluid velocity *below* the CAK point does not substantially differ from the one-component solution, the resulting mass-loss rate in the two-component case is almost the same as in the one-component case.

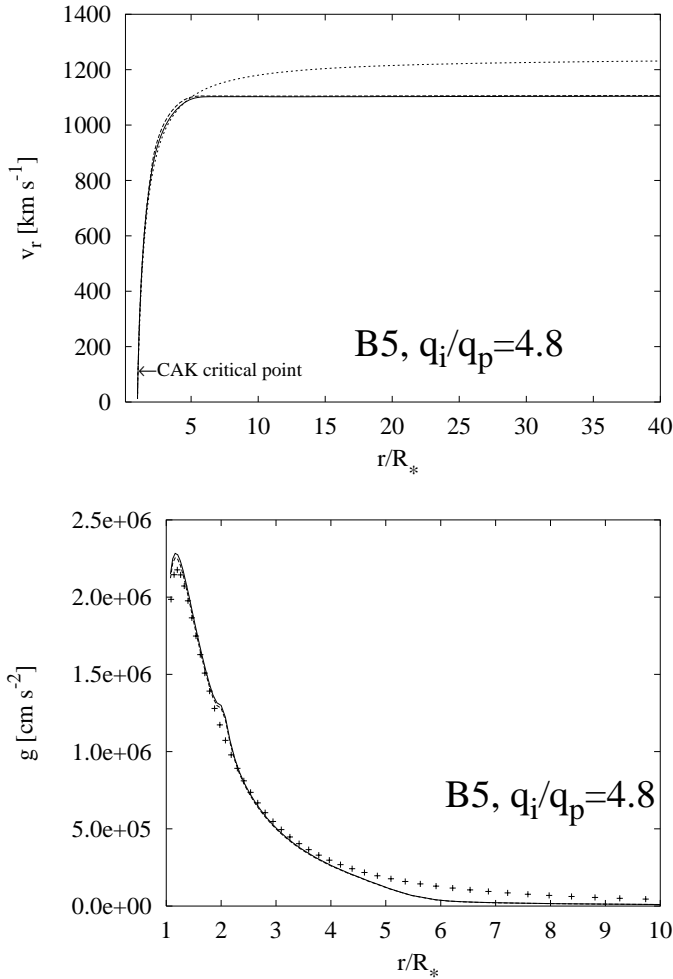


Fig. 5. The same as Fig. 2 for $q_i = 4.8 q_p$.

3.3. Limiting cases

The velocity profile that is displayed in Fig. 2 seems to be really surprising. In order to understand more our results we did some experiments with rather unrealistic parameters. First, we enhanced the frictional force. The easiest way to do this is to raise the ionic charge. Although the ionic charge for a B5 star is about $2q_p$, such artificial change can mimic higher interaction between the two gases. The result for a model with a ionic charge $q_i = 5q_p$ is in Fig. 4. The result is that was expected. Higher friction force causes the two gases behave as a one-component plasma, friction is able to transfer sufficient momentum from metals to the passive plasma throughout the wind. However, at the outer parts of the wind holds $x_{pi} \approx 1$. Consequently, lowering of the ionic charge (i.e. lowering of the friction force) would lead to the lowering of the outflow velocity gradient, and, finally, to lower terminal velocity, as is shown in Fig. 5 for the case of $q_i = 4.8$. In this case the frictional acceleration is fully balanced by the radiative acceleration in two-component model and corresponds to radiative acceleration in one-component model to radii $r \approx 4R_*$. Near this point Chandrasekhar function reaches its maximum ($x_{pi} \approx 1$) and metallic component is not able to

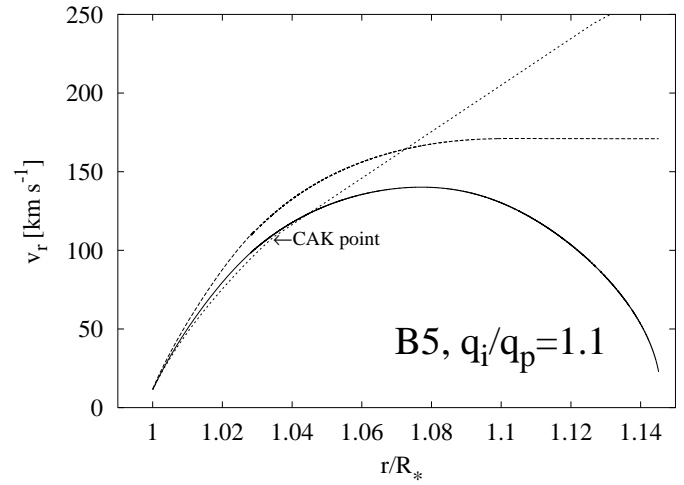


Fig. 6. The same as the upper panel of Fig. 2, but for $q_i = 1.1 q_p$. Note passive plasma velocity is lower than escape velocity everywhere (see Fig. 2).

transfer sufficient amount of momentum to passive plasma as in one-component case.

In our second experiment, we lowered the friction force using the same method, namely we lowered the ionic charge to the value $q_i = 1.1 q_p$. The result is displayed in Fig. 6. We see that the two components decouple *below* the critical point. Since the velocity of a passive plasma (hydrogen) is lower than the escape velocity, the latter must fall back on the stellar surface. In this case $r < r_c$ and passive plasma solution is of the type (5) – see Fig. 15.1 in Mihalas (1978). Similar effect of reaccretion was studied by Porter & Skouza (1999). For such a low values of q_i hydrostatic solution for passive plasma and wind solution for absorbing ions exists as shown by Babel (1996).

3.4. The possibility of ion decoupling

Our results are in contradiction to the generally accepted idea of ion decoupling in multicomponent stellar winds (Springmann & Pauldrach 1992, Porter & Drew 1995, Porter & Skouza 1999). It is therefore worth obtaining a deeper insight into the problem. To do this, we assumed that the line force does not depend on the *gradient* of the velocity. Assuming this, we rewrite the Eq. (25) in the form

$$\Delta \frac{dv_{ri}}{dr} = \frac{1}{\rho_i} \frac{\Delta R_{pi}}{v_{ri}}. \quad (26)$$

Since $\Delta R_{pi} > 0$, it follows that $\Delta (dv_{ri}/dr)$ is positive even if the gradient dv_{rp}/dr decreases due to the lowering of frictional force. This means that the components would decouple if the radiative force does not depend on the velocity gradient.

4. Discussion

Our new simple hydrodynamic calculations showed that for specific conditions friction does not lead to total decoupling of the radiatively accelerated ions in stellar wind. Similar calculations

for the case of the coronal wind and hydrogen and helium gases (of course without radiative acceleration) were performed by Bürgi (1992). He computed a three-component model of the coronal wind with inclusion of friction and he found that protons and alpha particles do not decouple for the case of a coronal wind. Inspecting his Fig. 3. we can infer that there is a difference between velocities of both components for some maximum temperature. Farther in the wind velocities of both components approach each other and do not decouple.

We found an abrupt decrease of the outflow velocity with respect to one-fluid description. This effect depends essentially on the mass-loss rate, the higher mass loss rate, the lower it is. Consequently, it is stronger for later B stars and weaker for earlier B stars. It is completely missing for O stars.

The lowering of the terminal velocity found by us is a consequence of the CAK force (which depends on the velocity gradient) and the interaction between wind components. If the driving force did not depend on the velocity gradient, decoupling would occur.

Two of our assumptions deserve further investigation, namely neglecting electrons and the isothermicity of the wind. Electrons may transfer momentum from metals to the passive plasma and thus modify the effect. On the other hand, allowing heating or cooling of the wind may lead to decoupling of individual metals. However, this possibility needs verification by detailed calculations. Both these assumptions will be relaxed in future calculations and the results together with the detailed equations will be published in our future paper.

Finally, we mention the measurements of v_∞ for a large sample of stars by Lamers et al. (1995). They found a sudden drop of v_∞ near $T_{\text{eff}} = 21000$ K with respect to earlier stars. Note, that this drop corresponds to the decreasing of the terminal wind velocity found by our simple calculations. This gives an alternative to the interpretation by Vink et al. (1999), who used the model of a bistable wind of Pauldrach & Puls (1990).

Acknowledgements. The authors would like to thank Drs. John Porter and Stanley Owocki for their critical comments of the manuscript. This research has made use of NASA's Astrophysics Data System Abstract Service. This work was supported by a grant of the Grant Agency of the Academy of Sciences of the Czech Republic A3003805, and by projects K1-003-601/4 and K1-043-601.

Appendix A: details of the numerical method

Individual members of the operator \mathbf{P} in Eq. (15) are the following:

– boundary conditions

$$P_1 = \rho_{i1} - \rho_0 \quad (\text{A.1a})$$

$$P_2 = \frac{2a_p^2}{r_1} + \mathcal{R}_{p1} \ln \Lambda + \frac{G\mathfrak{M}}{r_1^2} (1 - \Gamma) \quad (\text{A.1b})$$

$$P_3 = \rho_{p1} - \frac{1}{\mathfrak{M}_i} \rho_{i1} \frac{v_{ri1}}{v_{rp1}} \quad (\text{A.1c})$$

$$P_4 = v_{rp1} - a_p \quad (\text{A.1d})$$

– continuity and momentum equations

$$P_{4i-7} = \left[\frac{d(r^2 \rho_i v_{ri})}{dr} \right]_i \quad (\text{A.2a})$$

$$P_{4i-6} = \bar{v}_{ri,i} \left[\frac{dv_{ri}}{dr} \right]_i + \frac{a_i^2}{\bar{\rho}_{i,i}} \left[\frac{d\rho_i}{dr} \right]_i + \frac{G\mathfrak{M}}{\bar{r}_i^2} (1 - \Gamma) - x_\alpha \left(\frac{1}{\bar{\rho}_{i,i}} \left[\frac{dv_{ri}}{dr} \right]_i \right)^\alpha + \mathcal{R}_{ip} \ln \Lambda \quad (\text{A.2b})$$

$$P_{4i-5} = \left[\frac{d(r^2 \rho_p v_{rp})}{dr} \right]_i \quad (\text{A.2c})$$

$$P_{4i-4} = \bar{v}_{rp,i} \left[\frac{dv_{rp}}{dr} \right]_i + \frac{a_p^2}{\bar{\rho}_{p,i}} \left[\frac{d\rho_p}{dr} \right]_i + \frac{G\mathfrak{M}}{\bar{r}_i^2} (1 - \Gamma) + \mathcal{R}_{pi} \ln \Lambda \quad (\text{A.2d})$$

where

$$\bar{X}_i = \begin{cases} X_i, & i < NR, \\ \frac{1}{2} (X_i + X_{i-1}), & i = NR, \end{cases} \quad (\text{A.3a})$$

$$\left[\frac{dX}{dr} \right]_i = \begin{cases} y_i \frac{X_{i+1} - X_i}{\Delta r_{i+1}} + (1 - y_i) \frac{X_i - X_{i-1}}{\Delta r_i}, & i < NR, \\ \frac{X_i - X_{i-1}}{\Delta r_i}, & i = NR, \end{cases} \quad (\text{A.3b})$$

where X stands for $r, v_{ri}, v_{rp}, \rho_i, \rho_p$

$$\Delta r_i = r_i - r_{i-1}, \quad (\text{A.3c})$$

$$y_i = \frac{r_i - \bar{r}_i}{\bar{r}_{i+1} - \bar{r}_i}, \quad (\text{A.3d})$$

$$\mathcal{R}_{ab} = \bar{\rho}_b \frac{4\pi q_a^2 q_b^2}{m_a m_b k T} \frac{\bar{v}_{ra} - \bar{v}_{rb}}{|\bar{v}_{ra} - \bar{v}_{rb}|} G(\bar{x}_{ab}) \quad (\text{A.3e})$$

where a, b , stands for i, p

$$\ln \Lambda = \ln \left(24\pi \sqrt{\frac{m_p}{2\bar{\rho}_{p,i}}} \left(\frac{kT}{4\pi e^2} \right)^{3/2} \right) \quad (\text{A.3f})$$

$$x_\alpha = \frac{\sigma_e L}{4\pi r^2 c} \left(\frac{1}{10^{11} \text{cm}^{-3}} \frac{\bar{\rho}_i}{m_p W} \right)^\delta \times \frac{(1 + \bar{\sigma}_i)^{\alpha+1} - (1 + \bar{\sigma}_i \mu_c^2)^{\alpha+1}}{(\alpha + 1) (1 - \mu_c^2) \bar{\sigma}_i (1 + \bar{\sigma}_i)^\alpha} k (\sigma_e v_{\text{th}})^{-\alpha} \quad (\text{A.3g})$$

$$\bar{\sigma}_i = \left[\frac{dv_{ri,i}}{dr} \right]_i \frac{\bar{r}_i}{\bar{v}_{ri,i}} - 1 \quad (\text{A.3h})$$

$$\mu_c = \sqrt{1 - \left(\frac{R_*}{\bar{r}_i} \right)^2} \quad (\text{A.3i})$$

where i denotes i -th point of the grid.

References

- Abbott D.C., 1980, ApJ 242, 1183
- Abbott D.C., 1982, ApJ 259, 282
- Babel J., 1995, A&A 301, 823
- Babel J., 1996, A&A 309, 867
- Braginskij S.I., 1963, in: Leontovich M.A. (ed.), Voprosy teorii plazmy 1, Moskva: Gosatomizdat, p. 183

- Bürgi A., 1992, *J. Geophys. Res.* 97, 3137
- Castor J.I., Abbott D.C., Klein R.I., 1975, *ApJ* 195, 157 (CAK)
- Castor J.I., Abbott D.C., Klein R.I., 1976, in: Cayrel R., Sternberg M. (eds.), *Physique des mouvements dans les atmosphères stellaires*. Paris: CNRS, p. 363
- Dreicer H., 1959, *Phys. Rev.* 115, 238
- Friend D.B., Abbott D.C., 1986, *ApJ* 311, 701
- Harmanec P., 1988, *Bull. Astron. Inst. Czechosl.* 39, 329
- Heney L.G., Forbes J.E., Gould N.L., 1964, *ApJ* 139, 306
- Hunger K., Groote D., 1999, *A&A* 351, 554
- Krtička J., Kubát J., 2000, in: Lamers H.J.G., Sagar A.E. (eds.), *Thermal and ionization aspects of flows from hot stars: observations and theory*, ASP Conf. Ser. 204, p. 235
- Lamers H.J.G., Snow T.P., Lindholm D.M., 1995, *ApJ* 455, 269
- Mihalas D., *Stellar Atmospheres*, 1978, San Francisco: Freeman & Co.
- Nobili L., Turolla R., 1988, *ApJ* 333, 248
- Pauldrach A., Puls J., 1990, *A&A* 237, 409
- Pauldrach A., Puls J., Kudritzki R.P., 1986, *A&A* 164, 86
- Porter J.M., Drew J.E., 1995, *A&A* 296, 761
- Porter J.M., Skouza B.A., 1999, *A&A* 344, 205
- Springmann U.W.E., Pauldrach A.W.A., 1992, *A&A* 262, 515 (SP)
- Vink J.S., de Koter A., Lamers H.J.G., 1999, *A&A* 350, 181